Waveguide Bending Design Analysis

Theory of Bending and Formulae for Determination of Wall Thicknesses

By F. J. FUCHS, JR.

(Manuscript received June 4, 1959)

The art of rectangular tube bending is analyzed, with particular attention being given to tube wall thickness variations. Effects of these variations on tool design are discussed, and methods and formulae for determination of wall distortions are presented.

1. INTRODUCTION

For many years, waveguide bends for most microwave installations have been difficult and expensive to produce. The art of tube bending was not sufficiently advanced to make economically possible the extremely close tolerances required in waveguides. This was true even when waveguides were first introduced into radar equipment. It later became evident, as increased power, higher aircraft speeds and missile applications made waveguide requirements more severe, that the bending technique would have to be improved. First, a faster method of bending had to be found, since the best of existing methods required about 30 minutes to make one bend. Second, to reduce transmission losses, the new method had to produce bends that met closer internal cross-sectional tolerances. Third, bends of much smaller radius, more closely spaced compound bends and bends adjacent to swaged and twisted sections had to be made to meet new design demands. In addition to these specific improvements and innovations in the bending technique, production uniformity was desirable, since it is only through uniformity that statistical quality control can be realized.

At the Western Electric North Carolina Works the development of waveguide bending began in 1951 and continued for the next five years. This article describes the new bending process and indicates how internal cross-sectional accuracy is maintained despite material flow due to the bending action that changes the tubing's external dimensions. This in-

formation is of paramount importance to the bending tool designer and can also greatly aid the waveguide component designer who may wish to apply assembly details or machining in the region of the bend where wall thickness changes.

The several methods of bending that existed prior to this development are briefly reviewed. One of these, draw bending, is explained in somewhat more detail, because it was chosen as the basic method on which the improved technique was developed. The tooling used is shown and explained to acquaint the reader with terms used later in the analysis of effects of wall distortions on bend accuracy.

The material flow patterns and cross-sectional distortions are shown qualitatively and related to the individual tool parts. Corrective contouring evolves from these relationships to compensate for such distortions. Then, methods and formulae are advanced to make it possible to calculate accurately the wall thickness changes at any point in the bend region. For several of the more common sizes of waveguide, graphs are presented for reference in designs in which wall thickness must be evaluated.

Most of the formulae used in this discussion contain empirical constants. Therefore, an Appendix is given to explain the derivation of equations and provide supporting data for the constants.

II. TUBE BENDING METHODS

All tube bending methods consist basically of filling a tube with something to prevent its natural tendency to collapse and then bending it around a form, meanwhile constraining the outside of the tube by various methods to keep it from losing shape. There are three common methods of tube bending, all of which have been used to bend waveguides: compression bending, form bending and draw bending.

In compression bending, as shown in Fig. 1, the tube is filled with a close-fitting mandrel, laminated strips, low-melting-point alloy or other material. Then one end of the tube is clamped against a form die and the other end is wrapped around the curved portion of the die.

In form bending a filler is placed in the tube, and the bend is made by use of a punch and die in a manner similar to that employed in a sheet metal press brake. The tube is constrained at its sides by plates mounted on the form die.

These two methods of bending require a filler that is free to bend but will hold the cross section of the waveguide to close tolerance. A soft metal filler (lead, for example) will bend, but it cannot preserve the accuracy of cross section. Laminated strip filler will both bend readily

and maintain cross section, but it is extremely difficult to load and unload. Also, edges of the laminations mar the sidewalls of the tube. The link-type mandrel filler works well for large-radius bends in thick-walled tubing, but in thin-walled waveguide the tube wall tends to "oil can" in between the links, as shown in Fig. 2. These are the problems that make form and compression bending impractical for economical, accurate waveguide bends.

The third common tube bending method is draw bending, illustrated in Fig. 3. Fig. 4 is a photograph of a typical draw bending tool.

It can be seen that this process is very similar to compression bending, and the tooling is almost identical. The important difference is that the tube is clamped against the straight portion of the form die and both are rotated, thus pulling the tube through the wiper and pressure dies

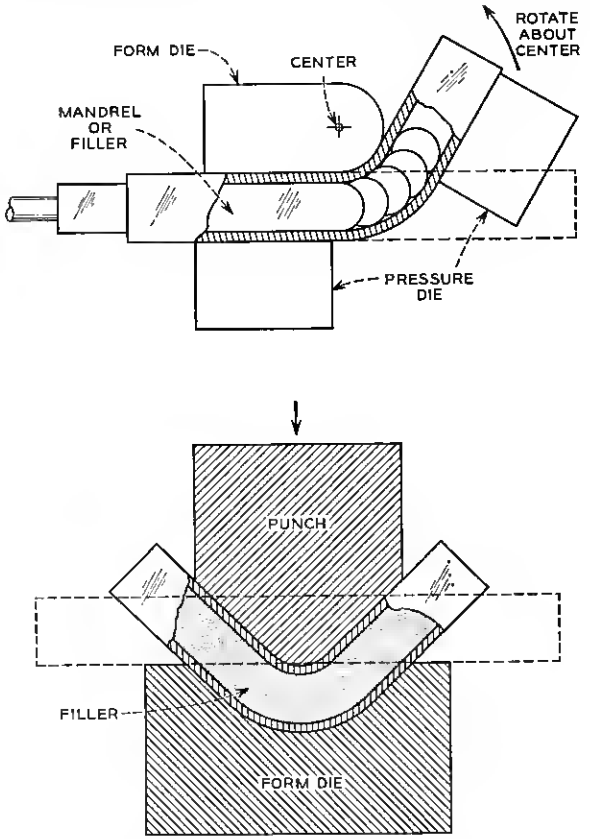

Fig. 1 — (a). Compression bending; (b) form bending.

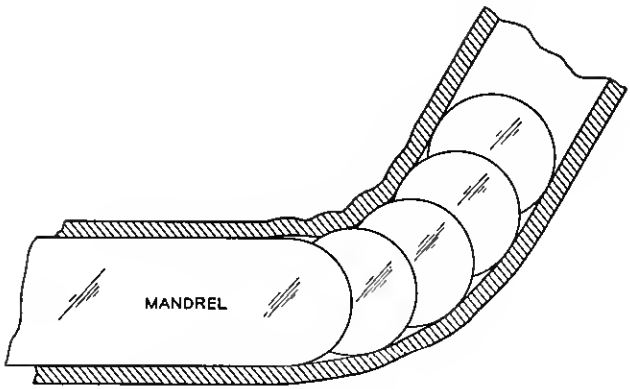

Fig. 2 — Nondrawing bending operation.

as it wraps around the curved form. This makes possible a drawing action of the tube over the mandrel, which prevents the tube wall from buckling because it is being "ironed" by the mandrel links.

When the draw bending process was selected to develop waveguide bending, many improvements had to be made to meet the problems presented. Distortion of the tubing exerted such extreme forces on the mandrel links that breakage was prohibitive on all but very large radius bends. Thin walls of waveguide wrinkled in almost every case, and no mandrels were available to make compound bends. Another fault more pronounced in draw bending is tube breakage on small radius bends, where pulling action subjects the tube to more axial tension. One way

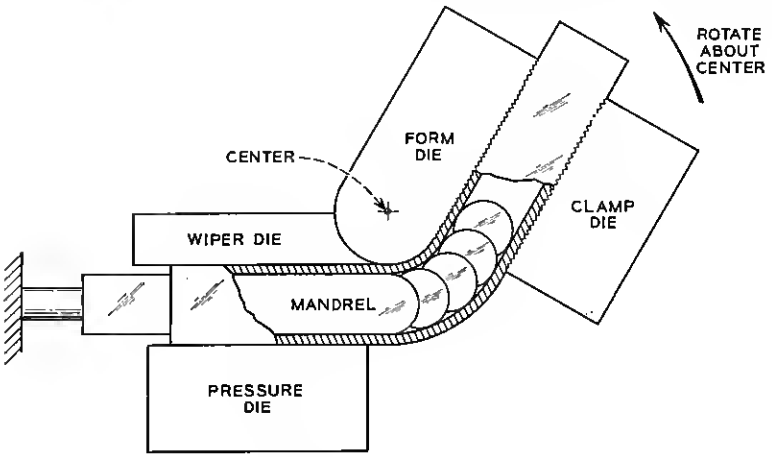

Fig. 3 — Draw bending.

Fig. 4 — A typical bending die.

of preventing this breakage is to employ a "booster" to compress the tube axially as it is bending. However, boosting, while decreasing the tensile forces, increases the wall build-up. Fig. 5 illustrates this effect. These are the specific problems that were the main targets of the development work.

III. REFINING THE DRAW BENDING TECHNIQUE

Now it will be shown how the draw bending technique is refined to give satisfactory performance.

Wall distortions are obviously detrimental to accurate tube bending,

but the nature of the process (the necessary application of tensile forces to the outside wall and compressive forces to the inner wall) makes it impossible to eliminate wall distortion. Assuming that the next best thing to elimination is accommodation, it appears that bending tools might be modified to allow for wall build-up in such a way that an accurate internal tube cross section could be preserved. Fig. 6 shows a bend being formed in the tool. The inner wall of the tube, which lies against the wiper and form die, tends to thicken, due to the compressive force involved in the bend. Designs of these parts of the tool are critical, because they must prevent buckling under great pressures. The top and bottom walls of the tube bend thicken toward the inner radius and become thinner at the outer radius. Therefore, the top and bottom plates must prevent the inner parts of these walls from buckling, even though they do not even touch the plates at the outer parts of the walls. The outer portions of the bend are in tension and pull in against the mandrel, which must be strong enough to withstand the forces involved and accurate enough to maintain size.

After investigation of sample bends by cutting and measuring wall thickness at various points in and around the bent portion, a definite pattern of distortion was revealed, as shown in Fig. 7. The distortions do not end at the tangent lines, but extend outward along the straight ends in an elliptical shape, and the wall thickness varies within this pattern. Fig. 8 is a more dramatic illustration of wall distortion. It is a 152° bend made in $\frac{5}{8}$- by $1\frac{1}{4}$-inch waveguide on a die with $\frac{1}{2}$-inch radius.

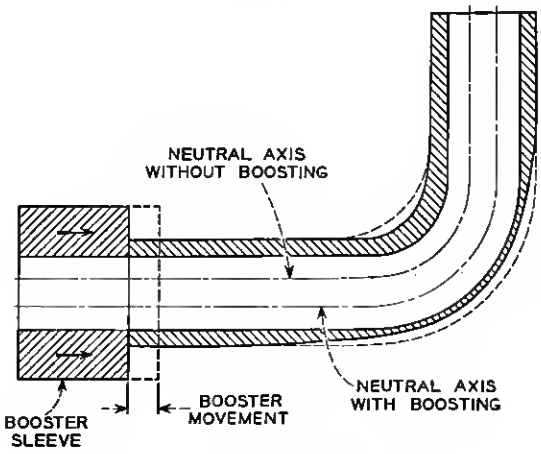

Fig. 5 — Effect of "boosting".

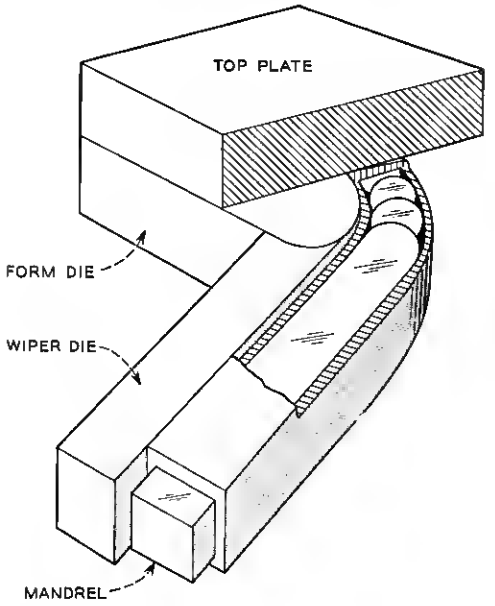

Fig. 6 — Wall distortions in relation to tooling.

These wall changes severely distort the cross section of the tube when an unrefined die is used. Fig. 9 shows what can happen, especially in small-radius bends. The thickening inner wall pushes the mandrel outward, and thus opens up a space behind the mandrel stem and allows the tube to wrinkle. The inner top and bottom walls thicken against the plates, moving them away from the form die and allow the top and bottom walls to bulge away from the mandrel. If the tooling and machinery is made extremely rigid in an attempt to prevent wrinkling and

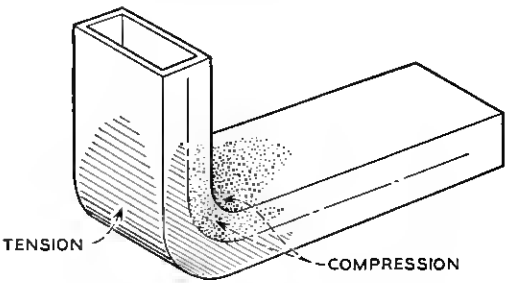

Fig. 7 — Distortion patterns in a bend.

Fig. 8 — Wall distortions in a typical "H" bend.

bulging (this is often done), the mandrel is severely crushed by the thickening walls of the waveguide, while the flexible links, limited in strength, break off. On the other hand, the tools can be carefully contoured to allow for wall build-up, and the tube can maintain its internal cross section and simply "grow" into the recesses provided in the dies.

Fig. 10 shows how this is done. The form die is made smaller in radius by the same amount as the wall thickens. The wiper die is tapered off at the end to match the tapered wall of the tube, and the straight portion of the form die at the clamp end is similarly tapered. Radially tapered recesses are cut into the top and bottom plates to match the wall changes there. This scheme was tried experimentally and proved to be successful when the contouring of the die was accurate in location and amount. The pressures against the tools were greatly relieved, and the internal dimensions of the tube were held accurately. However, in order to contour the dies to sufficient accuracy, a great deal of cut-and-try work was involved. Mathematical evaluation of wall distortions in amount and location thus arises as a practical design necessity, and is undertaken in the following section.

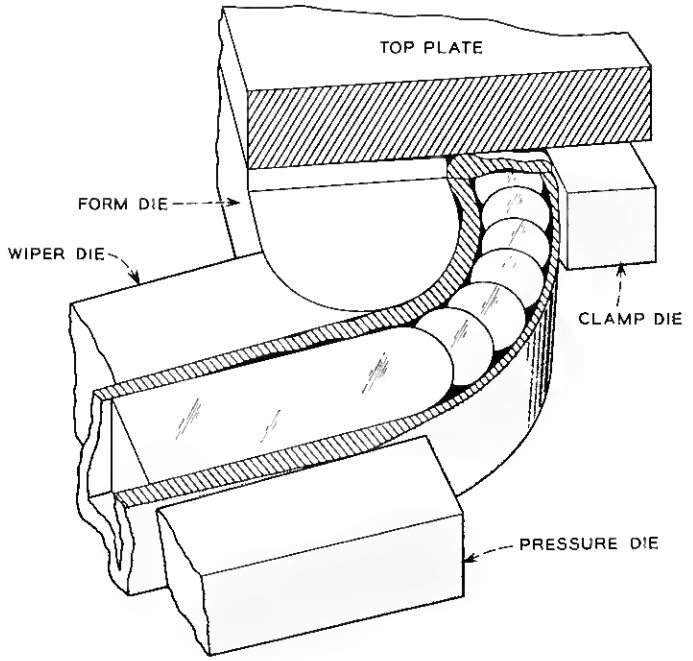

Fig. 9 — Wrinkles caused by wall distortions.

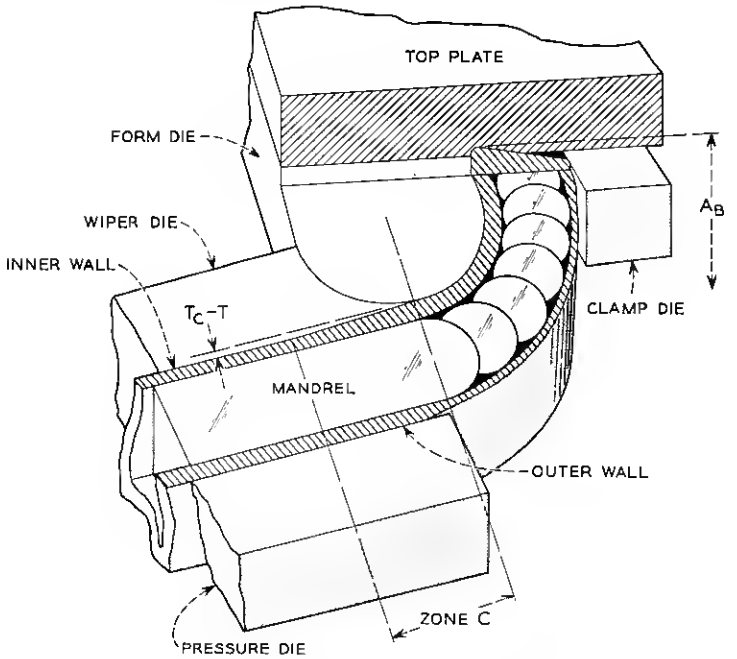

Fig. 10 — Die contoured to prevent wrinkling.

TABLE I — EQUATIONS FOR WALL THICKNESS CALCULATIONS–CONDITIONS I AND II

Condition I $0.0175\,\alpha\,(R_D + S - 0.5T) > S + A$ or $0.0175\alpha\,(R_D + 0.5T) > S + A$ (Special case: $T_{C1} - T = T - T_{T1}$)	Equation Number (See Appendix)
$T_C = -0.263H + \sqrt{0.069H^2 + \dfrac{0.526ATR_C}{R_D + 0.5T + 151S\left(\dfrac{R_D + 0.5T}{R_C}\right)^{0.564}}}$	(7)
$T_T = -0.263H + \sqrt{0.069H^2 + \dfrac{0.526ATR_C}{R_D + S - 0.5T}}$	(8)
$A_B = 0.5H + \sqrt{0.25H^2 + \dfrac{1.9ATR_C}{R_D + 0.5T + 0.151S\left(\dfrac{R_D + 0.5T}{R_C}\right)^{0.564}}}$	(9)
$A_T = 0.5\mathrm{H} + \sqrt{0.25H^2 + \dfrac{1.9ATR_C}{R_D + S - 0.5T}}$	(10)
Condition II $0.0175\,\alpha\,(R_D + 0.5T) < S + A$ or $0.0175\,\alpha\,(R_D + S - 0.5T) < S + A$	
$T_{C1} = T_C\sqrt{1 - \dfrac{[S + A - 0.0175\,\alpha\,(R_D + 0.5T)]^2(T_C{}^2 - T^2)}{T_C{}^2(S + A)^2}}$	(2)
$A_{B1} = H + (A_B - H)\cdot\sqrt{1 - \dfrac{[S + A - 0.0175\,\alpha(R_D + 0.5T)^2][(A_B - H)^2 - (2T)^2]}{(A_B - H)^2(S + A)^2}}$	(3)
$T_{T1} = 2T - (2T - T_T)\cdot\sqrt{1 - \dfrac{[S + A - 0.0175\,\alpha(R_D + S - 0.5T)]^2[(2T - T_T)^2 - T^2]}{(S + A)^2(2T - T_T)^2}}$	(4)
$A_{T1} = 2A - H - (2A - A_T - H)\cdot\sqrt{1 - \dfrac{[S + A - 0.0175\,\alpha(R_D - 0.5T)]^2[(2A - A_T - H)^2 - (A - H)^2]}{(S + A)^2(2A - A_T - H)^2}}$	(5)

IV. MATHEMATICAL EVALUATION OF WALL DISTORTIONS

For explaining the evaluation procedures worked out, the notation of the various quantities shown in Fig. 11 will be used.

In order to evaluate the changes in wall thickness due to cold-flow from the bending stresses, a large number of parts were cut open and measured at several points, and the quantities T_C, T_T, A_B and A_T were recorded. From analysis of these data a mathematical procedure for

accurate evaluation was derived. It was found that two basic conditions exist for bends due to variation in angle of bend and radius. Table I defines these two conditions and also provides equations to be used to calculate the dimensions needed. The two conditions are:

i. If the angle of bend, α, and radius of the midpoint of the inner wall thickness, $R_D + 0.5T$, are such that the arc length is larger than the sum of the two nominal dimensions of the waveguide, $S + A$, Condition I exists. In the formulae for this condition the angle of bend is not used, since the changes in wall thickness do not increase with further increase in bend angle.

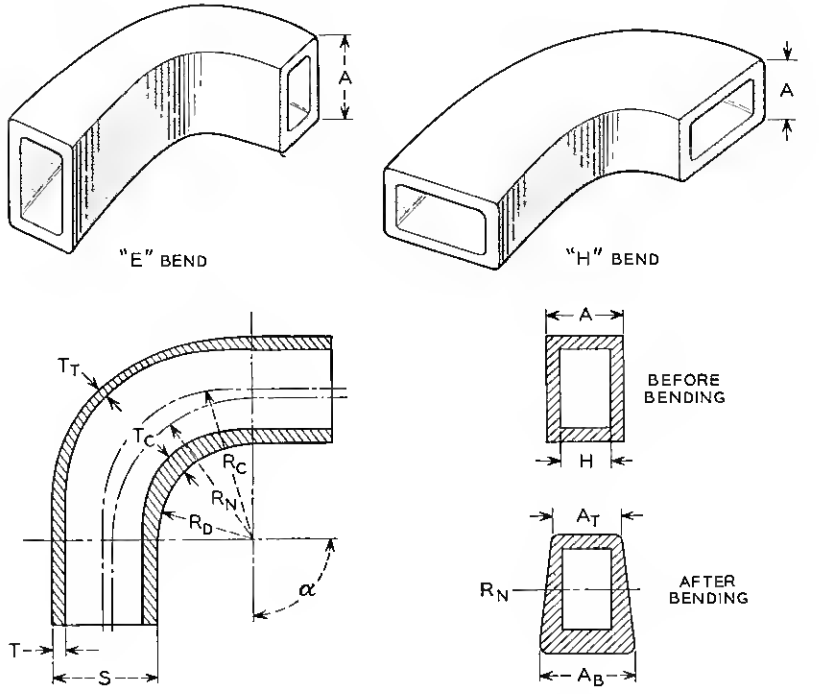

A - NOMINAL HEIGHT OF TUBE
A_B - HEIGHT OF TUBE AFTER BENDING
A_T - HEIGHT OF TUBE AFTER BENDING
H - HEIGHT OF TUBE INSIDE
T - NOMINAL WALL THICKNESS
T_C - MAXIMUM WALL THICKNESS AFTER BENDING
T_T - MINIMUM WALL THICKNESS AFTER BENDING
R_C - CENTERLINE RADIUS
R_D - RADIUS OF FORM DIE
R_N - RADIUS OF NEUTRAL AXIS
S - NOMINAL WIDTH OF TUBE
α - ANGLE OF BEND IN DEGREES

Fig. 11 — Definitions of terms used in waveguide bend analysis.

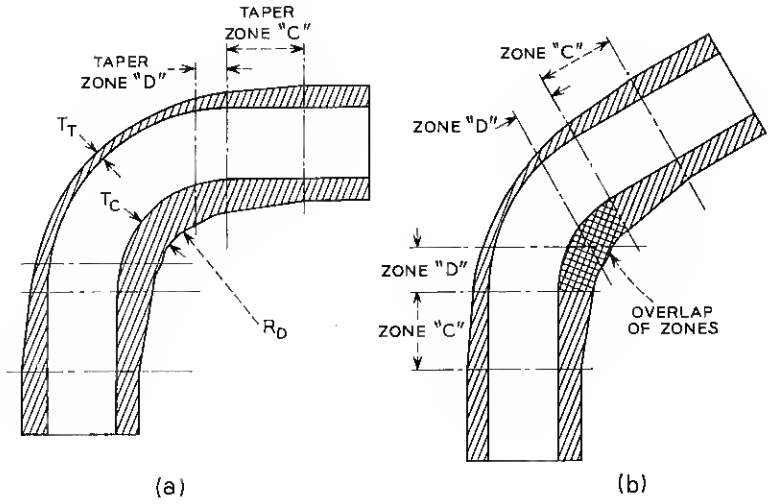

Fig. 12 — Variation of wall build-up with angle of bend.

ii. If the radius of die, R_D, and angle α are such that the arc length $(\pi/180)\alpha(R_D + 0.5T)$ is less than $S + A$, Condition II exists. Here the wall thickness changes are increasing with angle and, therefore, α is used in the calculation. Fig. 12 displays Conditions I and II.

The equations shown are partly analytical and partly empirical; their derivation and verification appears in the Appendix. By use of these calculations a series of graphs has been prepared for quick reference in determining wall thickness values. Figs. 13, 14 and 15 are examples of these graphs. They are based on the assumption that the neutral axis is located such that the outer wall thins down an amount equal to $T_C - T$. This is a condition that normally exists when a standard booster is used or when the form die radius is large enough to make the booster unnecessary.

There are several uses for these charts and evaluation procedures. In the case of new designs of bends, it is desirable to determine whether the bend can be made without breaking the tube, and how much distortion can be expected. The wall-thickness values may be needed to determine the feasibility of assembling details (such as tuning slugs, soldered brackets or clamps) to the guide in the vicinity of the bend. In compound bends, design specifications of the bend spacing can be affected by the wall thickness changes. These points are often overlooked in waveguide designs. In the design of tools for bending, as has already

been discussed, these wall thickness dimensions are essential. The following example will serve to illustrate the use of these data.

A new "H"-plane bend is to be designed out of ½- by 1-inch copper waveguide with an 0.050-inch wall thickness. The center line radius is 1.5 inches (nominal 1-inch form die radius), and the angle of bend is to be 180°. To determine if the bend can be made by standard procedures, it is necessary to know how thin the outer wall, T_T, will become, using standard tooling. For annealed copper, the maximum elongation before rupture is 30 to 35 per cent. Therefore, the wall thickness cannot decrease by more than 30 per cent of 0.050, down to 0.035 inch, or the tube will probably split. To determine which condition and thus which formula to use, it is necessary to calculate $(\pi/180)\alpha(R_D + 0.5T)$: in this case, 3.15. Consequently, the arc length is greater than $S + A$,

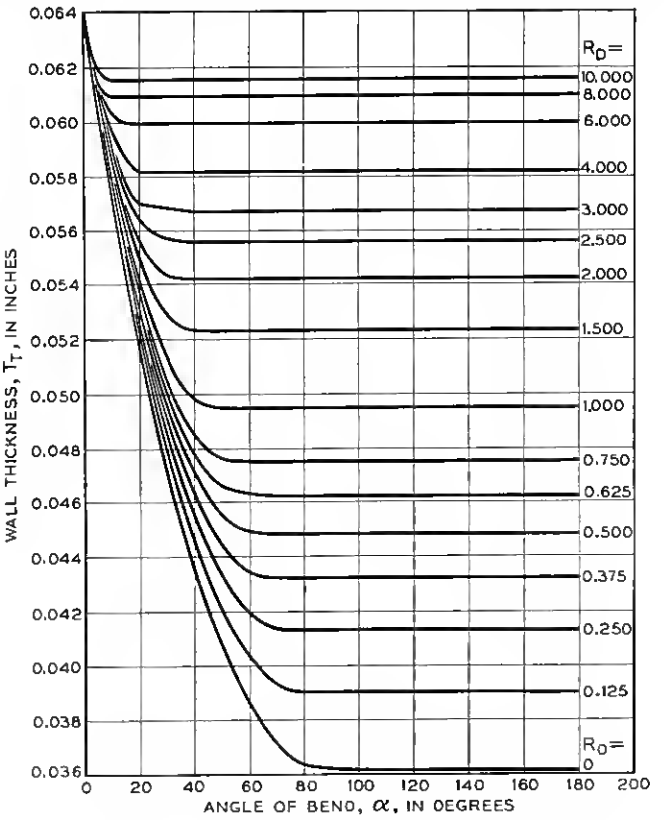

Fig. 13 — Wall thickness, T_T, vs. angle of bend.

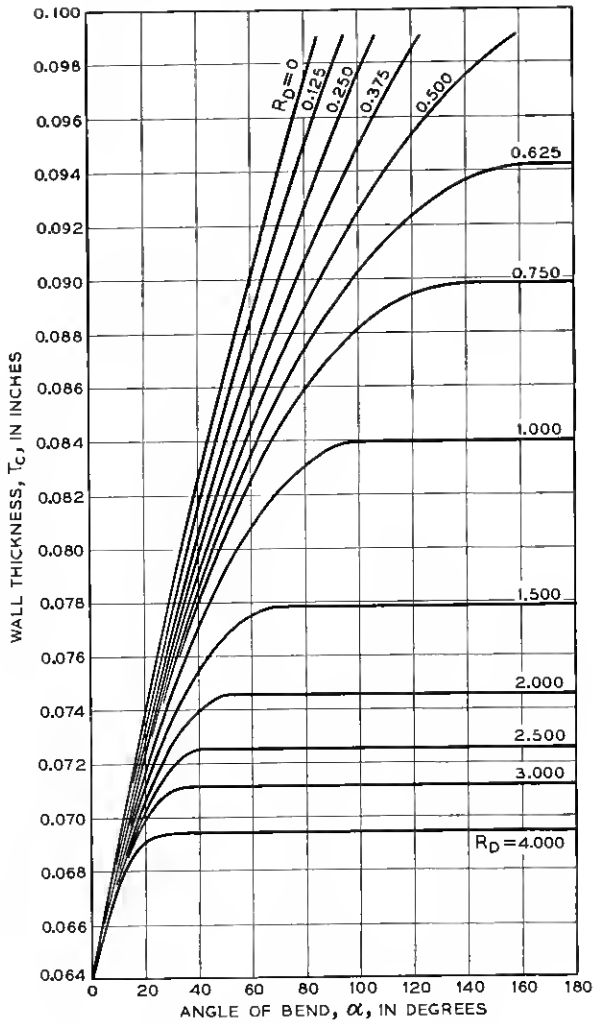

Fig. 14 — Wall thickness, T_C, vs. angle of bend.

(1.5 inches), and Condition I can be used for calculations. By substituting the proper values into the formulae in Table I for the given bend, the three dimensions T_C, T_T and A_B are determined:

$$T_C = 0.063 \text{ inch},$$

$$T_T = 0.037 \text{ inch},$$

$$A_B = 0.521 \text{ inch}.$$

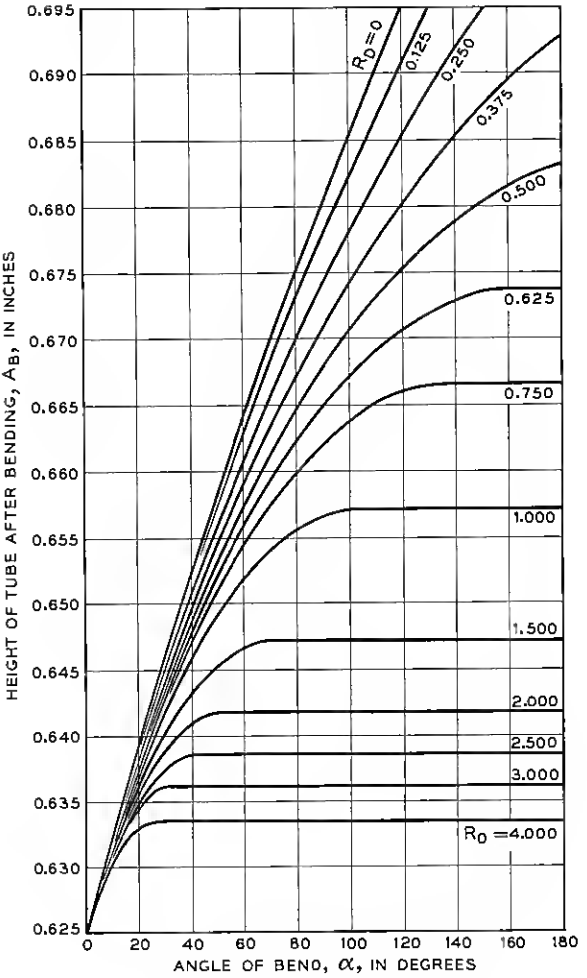

Fig. 15 — Height of tube vs. angle of bend.

Since T_T is greater than 0.035 inch no rupture will occur and the bend can be made economically.

The wall thickness that might be needed for assembly purposes is available from this same calculation. It should be noted, however, that the side wall thickness, $A_B - H/2$, is measured only at the form die radius, and tapers down to the nominal value at the neutral axis and to a proportional amount at the outer radius (refer to Fig. 11). Also, in the vicinity of the tangent lines of the bend the wall thicknesses taper

from those calculated (T_T, T_C) down to nominal in zones, as shown in Fig. 12(a). If the exact values are needed in these regions simple proportions can be used, because the variations are, for all practical calculations, straight tapers. The wall thickness at the center line of the bend is increased or decreased close to three-fourths of the maximum distortion and tapers into the straight portion of the tube for a distance that may be evaluated as $S + A$. At the end of this distance, the wall thickness resumes its original value. These same data are used to contour the tools to afford the accuracy required for the particular bend. The nominal 1-inch form die radius is ground undersize an amount equal to $T_C - T$, or 0.013 inch, for the build-up. The straight clamping portion of the form die is tapered from the tangent point for a distance of $S + A$ to reflect the tapered wall at the clamp end, and the wiper die tip is tapered similarly. Now the inner wall of the tube can thicken naturally and exert no undue pressures on the mandrel (see Fig. 10). The top and bottom plates are contoured to fit the side walls of the bend by means of a circular groove whose inside radius coincides with the 0.986-inch radius of the form die and whose outer radius coincides with the radius of the center line of the tube, in this case, 1.5 inches. The depth of this groove is 0.010 inch at the 0.986-inch radius and tapers to zero at the center line of the tube. These circular grooves hold the thickened portion of the sidewalls flat.

It should be noticed that the above contouring design is accurate for the bend only when the angle of bend is great enough so that Condition I exists. If the angle is small, the tube may be in Condition II, where the wall distortions are not fully developed, and, in order to preserve accuracy, a specially contoured die is used. However, in most cases the fully contoured die will produce a small-angle bend whose electrical performance is good.

In very small radius bends, the tools are not only contoured with nominal shapes as described, but they are also refined to reflect the elliptical pattern of distortion shown in Fig. 7. This is done by measuring a tube at several points after bending and tailoring the tools to fit. Since the above example was in Condition I, the angle of bend had little importance in build up, but, as the radius becomes smaller, the angle becomes more and more important. This is quite evident on inspection of Figs. 13, 14 and 15. The slope of each curve increases with decrease in R_D. In any design work, product or tooling, it becomes more important to recognize these wall distortions in smaller radius bends. Tool contouring must be done for smaller ranges of angles. To take the most extreme case — a zero radius bend — the die can be contoured and used

TABLE II — EQUATIONS FOR WALL THICKNESS CALCULATION—GENERAL CASE

General Case	Equation Number (See Appendix)
$T_C = -0.263H + \sqrt{0.069H^2 + \dfrac{0.526ATR_N}{R_D + 0.5T + 0.132(R_N - R_D - 0.5T)\left(\dfrac{R_D + 0.5T}{R_N}\right)^{0.2}}}$	(11)
$T_T = -0.263H + \sqrt{0.069H^2 + \dfrac{0.526ATR_N}{R_D + S - 0.5T - 0.132(R_D + S - 0.5T - R_N)\cdot\left(\dfrac{R_N}{R_D + S - 0.5T}\right)^{0.2}}}$	(12)
$A_B = 0.5H + \sqrt{0.25H^2 + \dfrac{1.9ATR_N}{R_D + 0.5T - 0.132(R_N - R_D - 0.5T)\left(\dfrac{R_D + 0.5T}{R_N}\right)^{0.2}}}$	(13)
$A_T = 0.5H + \sqrt{0.25H^2 + \dfrac{1.9ATR_N}{R_D + S - 0.5T - 0.132(R_D + S - 0.5T - R_N)\cdot\left(\dfrac{R_N}{R_D + S - 0.5T}\right)^{0.2}}}$	(14)

to bend no more than a 5° variation in angle to maintain an internal accuracy of 0.004 inch.

The equations shown in Table II are used in the same way as those in Table I. The necessity for two different systems of calculations, along with the method of derivation, is explained in the Appendix.

The charts shown in Figs. 13, 14 and 15 can be used for all bends whose outer walls lose as much in thickness as the inner wall gains, but if a small-radius bend is to be made, and the neutral axis must be boosted outward to prevent splitting, then the wall values must be computed for the specific case.

Perhaps it would be helpful to present such a case here. Assume a design involving quite a small radius — a $\frac{1}{2}$- by 1-inch waveguide with a 90° "H" bend and a 0.25-inch R_D. With this radius, Condition I calculations may be applied for the outer wall, since its length is less than $S + A$. To check the possibility of making the bend by standard proce-

dure the value T_T is calculated using (8). It is found to be 0.033 inch and, since this is less than the breaking point of 0.035 inch, special tooling will probably be necessary. Although the bend could be made by bending 45° and then annealing before finish-bending, this practice is undesirable, because it is more costly and produces a weaker product. A better procedure is to use the boosting principle to move the neutral axis outward until the wall thickness is greater than 0.035 inch. By substituting this value into (12) and solving for R_N, the new neutral axis position is found to be 0.778 inch. The neutral axis found using 0.033 inch for T_T was 0.732 inch. The difference, 0.046, is the amount of adjustment necessary for the booster. Now, by using 0.778 inch, any of the values can be determined from (11) and (7) for T_C and from (13) and (3) for A_B, and the tools can be accurately contoured.

Compound bends are often designed with close spacing between bends. When this spacing becomes less than the $S + A$ dimension of distortion beyond the bend, there is an overlap of stress patterns and the wall thickness at any point in this region must be computed for each bend; the resultant change in wall thickness at any point in that area will be the algebraic sum of the individual bend changes, a minus value for decreased wall and a plus value for a thickened wall. Usually, when the bends are spaced this closely, it is also necessary to hold the spacing quite accurately. This is reflected in centerline-to-centerline dimensional tolerances that often are less than ± 0.005 inch. Fig. 16 is an illustration of such a product. In designing dies to make the second bend for parts such as this it is necessary to provide a clamping nest that will support the first bend. This will prevent damage from the ensuing bending action and will accurately position the part to insure meeting of the desired centerline tolerance. The clamping nest must be contoured to

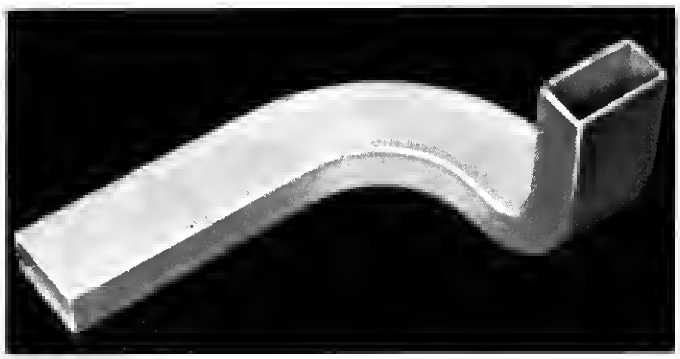

Fig. 16 — A close-coupled compound bend.

fit the first bend's wall distortions and the build-up of both bends must be allowed for in loeating the nest. Contouring of the nest can be readily prescribed from the eontours of the die used to make the first bend; these values are ealeulated as previously described. The distortions for the second bend are ealculated in the same manner, but the seetion of the die eorresponding to the place where overlapping distortions between the two bends oecur is dimensioned accordingly.

This product illustrated in Fig. 16 eonsists of an "E" and an "H" bend spaced 0.312 inch apart in $\frac{5}{8}$- by $1\frac{1}{4}$-tubing. The "E" bend has a eenterline radius of $\frac{3}{4}$ inch, and the "H" bend's centerline radius is 2 inehes. The centerline offset dimension required is 3.062 ± 0.005 inch.

Fig. 17 shows how the die for the product in Fig. 16 is contoured from the values taken from Figs. 13, 14 and 15. In addition to the contoured form die and top plate as shown, the elamp die is similarly faeed, and a eurved clamping block is used to baek up the outer wall of the nested bend. The subscripts 1 and 2 on the values in Fig. 17 refer to the nested bend and the second bend, respeetively.

V. CONCLUSION

These procedures and techniques developed in the waveguide bending project have had a marked effect on produetion eosts, quality and uniformity.

The cost of waveguide bends had been quite high, because of the

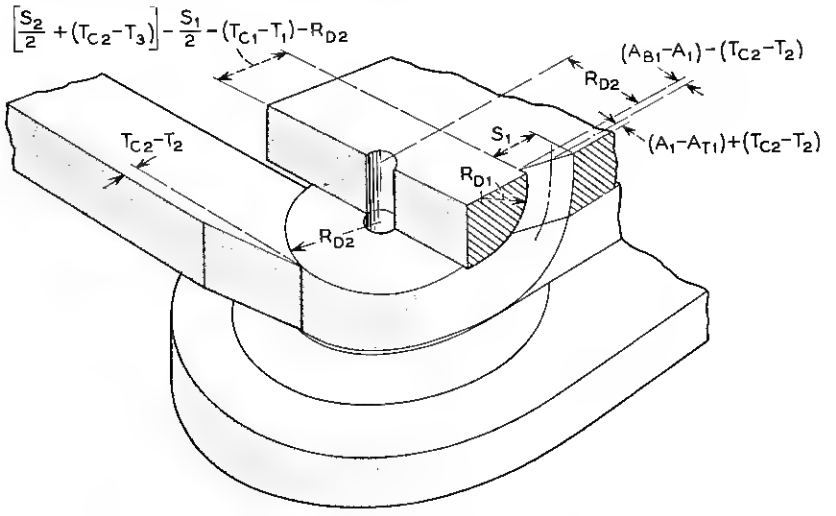

Fig. 17 — Die contours for a compound bend.

amount of labor involved in the loading and unloading of tube fillers and because of the very high spoilage rate. The new methods of contoured dies, permitting use of draw bending mandrels, have lowered the average cost of bends from over $7.00 to less than $2.00 each. Also, the capacity of the bending shop has increased tenfold per man hour.

Electrical transmission and physical appearance of the new bends are markedly improved. The elimination of hand work has considerably reduced surface scars and irregularities that not only were objectionable from a visual standpoint but also impaired electrical performance. It has been found that the uniformity of the process is reflected in an electrical performance from part to part which is exceptionally constant.

APPENDIX

This Appendix is used to explain the derivations of equations and present the experimental data used.

The basic method of computing wall thicknesses of bent tubing is to compare the length of the bent wall to the length of the neutral axis of the bend, and assume that the volume of the wall after bending is the same as it was before. The formula for T_C, Fig. 11, would be derived as follows:

Volume before bending:

$$V = \pi R_N \frac{\alpha}{180} AT.$$

Volume after bending:

$$V = \pi(R_D + 0.5T) \frac{\alpha}{180} A_B T_C.$$

Equating the two:

$$\pi R_N \frac{\alpha}{180} AT = \pi(R_D + .5T) \frac{\alpha}{180} A_B T_C.$$

Solving for T_C:

$$T_C = \frac{ATR_N}{(R_D + 0.5T)A_B}. \tag{1}$$

This basic calculation was made with two assumptions: first, that the distortion of the thickening wall ends abruptly at the two centerlines of bend; second, that wall increase is the same for any angle of bend. Neither of these conditions is found to be true, although the two are interrelated. It is found that the wall thickness changes beyond the tangent point of bend, as shown in Figs. 7 and 12. This distance beyond the centerline, Zone C, is approximately equal to $S + A$ in over-all

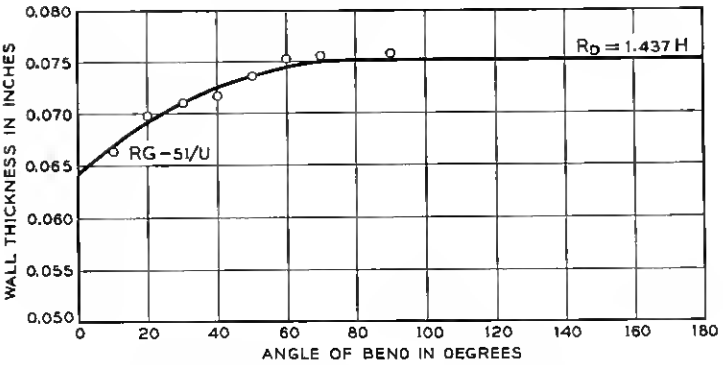

Fig. 18 — Wall thickness, T_c, for a typical bend.

length. Fig. 12 also shows a Zone D, which is in the bent portion of the waveguide. This zone is also reasonably constant in length, approximating $0.5(S + A)$. Since the wall distortion is a maximum at the end of Zone D and something less at the centerline of bend (found to be 0.75 of the maximum by experiment), it is evident that the wall thickness will change from nominal to its maximum value only after the bend has progressed sufficiently to provide an arc length, center to center, greater than $S + A$. Fig. 18, a curve of measured values for a typical bend, shows this effect clearly. The wall increases from nominal at 0° bend to a maximum at about 75° bend. For this inner wall, the angle of bend that gives an arc length of $S + A$, (1.875 inches in this case) is

$$\frac{(S + A)\ 180}{\pi(R_D + 0.5T)} = 73°.$$

In order to describe this build-up effect mathematically, use is made of the equation for an ellipse,

$$\frac{x^2}{a^2} + \frac{y^2}{b^2} = 1,$$

that fits the wall distortion curve very well. Referring to Fig. 19, b is equal to T_c at $X = 0$. At the known point of 0° bend, $X = S + A$ and $y = T$. By substituting these values into the general equation for an ellipse, the value a^2 can be found:

$$\frac{(S + A)^2}{a^2} + \frac{T^2}{T_c^2} = 1,$$

$$a^2 = \frac{(S + A)^2\ T_c^2}{T_c^2 - T^2}.$$

At any other point between $X = 0$ and $X = S + A$, X would be equal to the arc length of bend subtracted from $S + A$:

$$x = S + A - (R_D + 0.5T)\frac{\alpha\pi}{180}.$$

For the purpose of clarity, the value of y at this point is denoted T_{c1}. By substituting these values and the value of a^2 as above, the equation for an ellipse can be again rewritten:

$$\frac{\left[S + A - (R_D + 0.5T)\alpha\,\frac{\pi}{180}\right]^2}{\frac{(S + A)^2 T_c^2}{T_c^2 - T^2}} + \frac{T_{c1}^2}{T_c^2} = 1.$$

After solving for T_{c1}, the equation appears as:

$$T_{c1} = T_c \sqrt{1 - \frac{[S + A - 0.0175\alpha(R_D + 0.5T)]^2[T_c^2 - T^2]}{T_c^2(S + A)^2}}. \qquad (2)$$

This is the equation that was used for T_{c1} in Table II. The accuracy

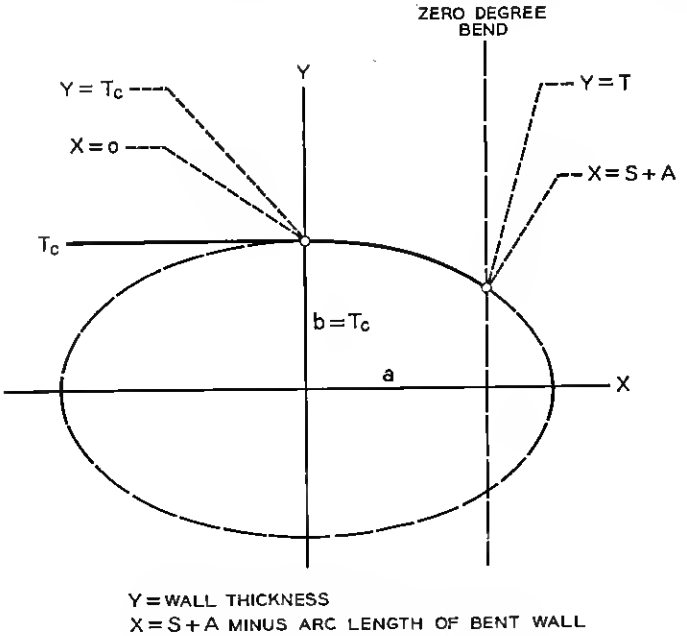

Fig. 19 — Ellipse used to derive equation (2).

of this calculation is within 0.002 inch on sizes of waveguide ranging from 0.391 by 0.702 inch to $1\frac{1}{2}$ by 3 inches. In Fig. 18 the curve shows the calculated values in relation to the experimental values for a typical bend.

The foregoing derivation was for the inner wall thickness only. The sidewall thickness is calculated in exactly the same way to evaluate the height of tube after bending, A_B. The only variation is that the calculated sidewall thickness is doubled and added to the internal height of the tube, H. This variation of (2) becomes

$$A_{B1} = H + (A_B - H) \cdot \sqrt{1 - \frac{[S + A - 0.0175\alpha(R_D + 0.5T)^2][(A_B - H)^2 - (2T)^2]}{(A_B - H)^2(S + A)^2}}. \quad (3)$$

Another value needed for bend analysis is the outer wall thickness, T_T. The same method of setting up an equation is used, with Zones C and D being the same length for tension as they are for compression. After solving the equation for the ellipse as shown in Fig. 20, the ex-

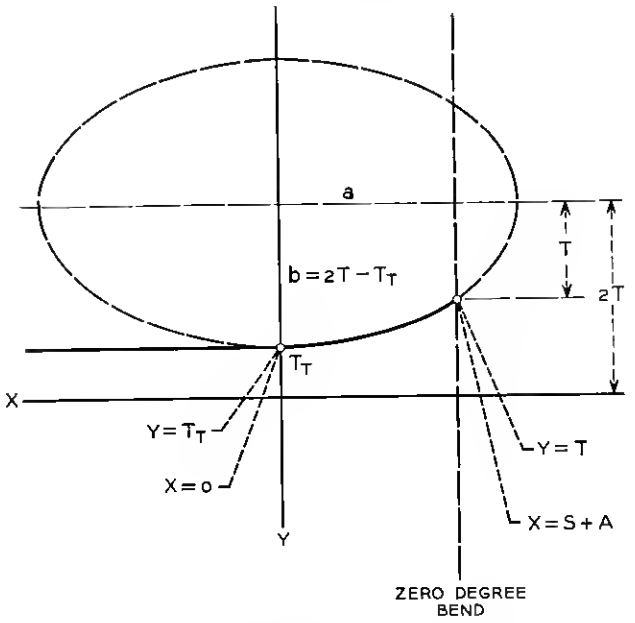

Fig. 20 — Ellipse used to derive equation (4).

pression for T_{T1} is as follows:

$$T_{T1} = 2T - (2T - T_T) \cdot \sqrt{1 - \frac{[S + A - 0.0175\alpha(R_D + S - 0.5T)]^2[(2T - T_T)^2 - T^2]}{(S + A)^2(2T - T_T)^2}} . \quad (4)$$

The only remaining value to determine is the height of tube after bending at the outer wall. This is derived from the same type of elliptical function as the foregoing, and is

$$A_{T1} = 2A - H - (2A - A_T - H) \cdot \sqrt{1 - \frac{[S + A - 0.0175(R_D - 0.5T)]^2 \cdot [(2A - A_T - H)^2 - (A - H)^2]}{(S + A)^2(2A - A_T - H)^2}} . \quad (5)$$

Equations (2), (3), (4) and (5) evaluate the wall distortions of a bend which is still in Condition II. The equations all include the values T_C, A_B, T_T and A_T, which must be determined first. Equation (1) expresses the wall distortions assuming no distortion beyond the bend. By rewriting the equation, the fact that the wall does thicken beyond the centerline is represented by an empirical addition to $(R_D + 0.5T)$. Measurements of samples which were boosted by standard methods were substituted into (6) and the value K was obtained:

$$T_C = - \frac{ATR_N}{A_B[(R_D + 0.5T) + K]} . \quad (6)$$

By assuming R_N equal to R_C and plotting K against various parameters, it was found that K equals

$$0.151S \left(\frac{R_D + 0.5T}{R_C} \right)^{0.564}$$

for T_C and close to zero for T_T. Therefore, equations for T_C and T_T appear as follows:

$$T_C = \frac{ATR_C}{A_B \left[R_D + 0.5T + 0.151S \left(\frac{R_D + 0.5T}{R_C} \right)^{0.564} \right]} ,$$

$$T_T = \frac{ATR_C}{A_T(R_D + S - 0.5T)} .$$

From Table III, it is evident that the sidewalls after bending assume a value close to 0.95 times their adjacent walls. From this, $A_B = H + 1.9T_C$ and $A_T = H + 1.9T_T$, and final equations for T_C and T_T can be

TABLE III — MEASUREMENTS OF WALL THICKNESSES TAKEN FROM SAMPLE PRODUCTION BENDS

Description of Bends	T_C	T_T	A_B	A_T	Ratio $\frac{A_B - H}{T_C}$	Ratio $\frac{A_T - H}{T_T}$
0.391 × 0.702 E, 0.196 R_D 90°	0.050	0.030	0.714	0.678	1.84	1.87
0.391 × 0.702 E, 0.562 R_D 150°	0.047	0.033	0.712	0.687	1.91	1.97
0.391 × 0.702 H, 0.351 R_D 90°	0.052	0.030	0.412	0.367	1.90	1.86
0.5 × 1 E, 0.5 R_D 90°	0.060	0.040	1.014	0.976	1.90	1.90
0.5 × 1 E, 0.348 R_D 90°	0.063	0.037	1.017	0.969	1.86	1.86
0.5 × 1 H, 0.625 R_D 90°	0.066	0.035	0.525	0.467	1.93	1.92
0.5 × 1 H, 0.625 R_D 180°	0.068	0.035	0.530	0.473	1.86	1.97
0.625 × 1.25 E, 1.5 R_D 180°	0.071	0.056	1.260	1.226	1.94	1.86
0.625 × 1.25 H, .5 R_D 90°	0.088	0.043	0.667	0.575	1.96	1.95
0.625 × 1.25 H, 0 R_D 45°	0.083	0.044	0.655	0.592	1.90	1.90
0.625 × 1.25 H, 1.5 R_D 90°	0.076	0.0523	0.640	0.587	1.88	1.91
0.625 × 1.25 H, 2 R_D 90°	0.075	0.053	0.645	0.593	1.95	1.86
1.273 × 2.418 E, 6.86 R_D 90°	0.069	0.059	2.423	2.399	1.93	1.85
1.273 × 2.418 H, 6.29 R_D 90°	0.073	0.056	1.285	1.250	1.92	1.88
Average					1.90	1.89

found by substituting $H + 1.9T_C$ and $H + 1.9T_T$ into the above and solving for the values T_C and T_T:

$$T_C = -0.263H + \sqrt{0.069H^2 + \frac{0.526ATR_C}{R_D + 0.5T + 0.151S\left(\frac{R_D + 0.5T}{R_C}\right)^{0.524}}}, \tag{7}$$

$$T_T = -0.263H + \sqrt{0.069H^2 + \frac{0.526ATR_C}{R_D + S - 0.5T}}. \tag{8}$$

The sidewall thicknesses A_B and A_T can be evaluated similarly:

$$A_B = H + \frac{1.9ATR_C}{A_B\left[R_D + 0.5T + 0.151S\left(\frac{R_D + 0.5T}{R_C}\right)^{0.564}\right]}.$$

Solving for A_B:

$$A_B = 0.5H + \sqrt{0.25H^2 + \frac{1.9ATR_C}{R_D + 0.5T + 0.151S\left(\frac{R_D + 0.5T}{R_C}\right)^{0.564}}}. \tag{9}$$

Similarly,

$$A_T = 0.5H + \sqrt{0.25H^2 + \frac{1.9ATR_C}{R_D + S - 0.5T}}. \tag{10}$$

These equations can be used to determine wall thicknesses within 0.002 inch for a range of waveguide sizes of from 0.391 to 2.418 inches and for any radius of bend.

Equations (7), (8), (9) and (10) can be used only where the tube wall distortions of outer and inner walls are almost equal. Fortunately, this is the normal situation, and these equations are very useful because they cover the great majority of cases. However, in cases where it is desirable to determine the neutral axis, R_N, or where R_N is known, it would also be desirable to have expressions for T_C, T_T, A_B and A_T in terms of R_N.

These expressions are written in general form as:

$$T_C = \frac{ATR_N}{A_B(R_D + 0.5T + K)},$$

$$T_T = \frac{ATR_N}{A_T(R_D + S - 0.5T - K)},$$

$$A_B = H + \frac{2ATR_N}{A_B(R_D + S - 0.5T - K)},$$

$$A_T = H + \frac{2ATR_N}{A_T(R_D + S - 0.5T - K)},$$

where K has the same significance as previously explained. By substitution of T_C and T_T taken from experimental samples in Table III and solving for R_N and K simultaneously, K is found to be equal to

$$0.132(R_N - R_D - 0.5T)\left(\frac{R_D + 0.5T}{R_N}\right)^{0.2}$$

and

$$0.132(R_D + S - 0.5T)\left(\frac{R_N}{R_D + S - 0.5T}\right)^{0.2}$$

for the respective cases.

Finally, T_C and T_T are evaluated by:

$$T_C = \frac{ATR_N}{A_B\left[R_D + 0.5T + 0.132(R_N - R_D - 0.5T)\left(\frac{R_D + 0.5T}{R_N}\right)^{0.2}\right]}.$$

Substituting $A_B = H + 1.9T_C$ and solving for T_C:

$$T_C = -0.263H + \sqrt{0.069H^2 + \frac{0.526ATR_N}{R_D + 0.5T + 0.132(R_N - R_D - 0.5T)} \cdot \left(\frac{R_D + 0.5T}{R_N}\right)^{0.2}}, \quad (11)$$

$$T_T = \frac{ATR_N}{A_T\left[R_D + S - 0.5T - 0.132(R_D + S - 0.5T - R_N) \cdot \left(\frac{R_N}{R_D + S - 0.5T}\right)^{0.2}\right]}.$$

Substituting $A_T = H + 1.9T_T$, and solving for T_T:

$$T_T = -0.263H + \sqrt{0.069H^2 + \frac{0.526ATR_N}{R_D + S - 0.5T - 0.132(R_D + S - 0.5T - R_N)\left(\frac{R_N}{R_D + S - 0.5T}\right)^{0.2}}}. \quad (12)$$

The sidewall thicknesses are found to be less than the outer and inner wall thicknesses. Table III shows this relationship to be a constant ratio: the sidewalls are 0.95 times the outer and inner walls. By use of this ratio, formulae for A_B and A_T are written as:

$$A_B = H + \frac{1.9ATR_N}{A_B\left[R_D + 0.5T + 0.132(R_N - R_D - 0.5T)\left(\frac{R_D + 0.5T}{R_N}\right)^{0.2}\right]}.$$

Solving for A_B:

$$A_B = 0.5H + \sqrt{0.25H^2 + \frac{1.9ATR_N}{R_D + 0.5T + 0.132(R_N - R_D - 0.5T) \cdot \left(\frac{R_D + 0.5T}{R_N}\right)^{0.2}}}. \quad (13)$$

Similarly,

$$A_T = H + \frac{1.9ATR_N}{A_T\left[R_D + S - 0.5T - 132(R_D + S - 0.5T - R_N)\left(\frac{R_N}{R_D + S - 0.5T}\right)^{0.2}\right]}.$$

Solving for A_T:

$$A_T = 0.5H + \sqrt{0.25H^2 + \frac{1.9ATR_N}{R_D + S - 0.5T - 0.132(R_D + S - 0.5T - R_N)} \cdot \left(\frac{R_N}{R_D + S - 0.5T}\right)^{0.2}} \quad (14)$$

Here, A_T and A_B have been shown as separate calculations, but where T_T and T_C are already known or computed A_T and A_B can be evaluated by:

$$A_T = H + 1.9T_T, \quad (15)$$

$$A_B = H + 1.9T_C. \quad (16)$$

These relations are found to be true for both Conditions I and II.